Title

Coastal upwelling drives ecosystem temporal variability from the surface to the abyssal seafloor.

Journal

Proceedings of the National Academy of Sciences of USA, 120(13)

Authors

Messié, Monique
Sherlock, Rob
Huffard, Christine
et al.

Publication Date

2023-03-28

DOI

10.1073/pnas.2214567120

Peer reviewed

PNAS RESEARCH ARTICLE | ECOLOGY

Coastal upwelling drives ecosystem temporal variability from the surface to the abyssal seafloor

Monique Messié[a,1], Rob E. Sherlock[a], Christine L. Huffard[a], J. Timothy Pennington[a], C. Anela Choy[a,b], Reiko P. Michisaki[a], Kevin Gomes[a], Francisco P. Chavez[a], Bruce H. Robison[a], and Kenneth L. Smith Jr.[a]

Edited by Edward DeLong, University of Hawai'i at Manoa, Honolulu, HI; received August 25, 2022; accepted February 10, 2023

Long-term biological time series that monitor ecosystems across the ocean's full water column are extremely rare. As a result, classic paradigms are yet to be tested. One such paradigm is that variations in coastal upwelling drive changes in marine ecosystems throughout the water column. We examine this hypothesis by using data from three multidecadal time series spanning surface (0 m), midwater (200 to 1,000 m), and benthic (~4,000 m) habitats in the central California Current Upwelling System. Data include microscopic counts of surface plankton, video quantification of midwater animals, and imaging of benthic seafloor invertebrates. Taxon-specific plankton biomass and midwater and benthic animal densities were separately analyzed with principal component analysis. Within each community, the first mode of variability corresponds to most taxa increasing and decreasing over time, capturing seasonal surface blooms and lower-frequency midwater and benthic variability. When compared to local wind-driven upwelling variability, each community correlates to changes in upwelling damped over distinct timescales. This suggests that periods of high upwelling favor increase in organism biomass or density from the surface ocean through the midwater down to the abyssal seafloor. These connections most likely occur directly via changes in primary production and vertical carbon flux, and to a lesser extent indirectly via other oceanic changes. The timescales over which species respond to upwelling are taxon-specific and are likely linked to the longevity of phytoplankton blooms (surface) and of animal life (midwater and benthos), which dictate how long upwelling-driven changes persist within each community.

coastal upwelling | California Current | ecosystem variability | animal lifespan | deep sea

Understanding how ecosystems respond to environmental forcing remains a fundamental challenge in marine science, particularly as the climate is changing (1–3). This task is complicated by a paucity of multidecade biological time series, especially taxonomic series that examine habitats spanning the full depth of the oceanic water column. Existing time series can provide information about response to environmental forcing (4), but often only describe communities within the upper 200 m, leaving over 95% of the world's ocean volume unexamined (5, 6). Moreover, taxonomic information remains limited as bulk properties are more easily measured. There is at present no published time series that monitors ecosystems from the ocean surface to the abyssal seafloor.

The Monterey Bay Aquarium Research Institute has supported three ecological time series in the California Current System starting in the late 1980s and continuing through 2022 (Fig. 1). Data for these series were collected independently, and represent the Monterey Bay photic zone (7), the Monterey Bay mesopelagic zone from 200 to 1,000 m (8), and a ~4,000-m abyssal seafloor habitat at the base of the Monterey deep-sea fan (9). They describe surface plankton, midwater gelatinous animals as well as some crustaceans, squids, and fishes, and benthic echinoderms. Due to their decades-long duration and focus on different habitats, these time series, here examined together for the first time, offer an unprecedented opportunity to investigate ecosystem variability over a range of temporal scales across the full water column and deep-sea benthos.

This approach is particularly important in the California Current System, a productive coastal upwelling ecosystem that sustains multiple fisheries and where improved knowledge of ecosystem drivers will benefit ecosystem-based management (10). Upwelling ecosystems are generally considered to be regulated from the bottom-up, with nutrient supply controlling phytoplankton populations, which in turn support intermediate and upper trophic levels (11–13). If so, biological variability is likely to be driven by physical processes controlling changes in nutrient supply. Upwelling, the process by which winds draws nutrient-rich, deep water into the sunlit surface layer, has been previously linked to phytoplankton, zooplankton, and pelagic ecosystem temporal variability (14–18). However, the biological impact of upwelling on the full ocean water column remains undetermined.

Significance

Drivers of marine ecosystem variability remain largely unknown, particularly beneath the euphotic zone where ecological measurements are difficult and rare. We examine ecosystem temporal variability in the highly productive California Current ecosystem, which is supported by seasonal coastal upwelling, a process in which wind draws nutrient-rich subsurface waters into the sunlit surface ocean. Bringing together three decades-long time series that have independently monitored surface, midwater, and abyssal benthic communities, we demonstrate that upwelling drives biological temporal variability from the surface to the abyssal seafloor. Our study supports a previous hypothesis that biological populations damp environmental fluctuations over timescales related to animal lifespans. Identifying these timescales may thus provide clues on animal lifespans, a valuable and often unknown biological parameter.

Author contributions: M.M., F.P.C., B.H.R., and K.L.S. designed research; M.M. performed research; F.P.C., B.H.R., and K.L.S. contributed new datasets; M.M., R.E.S., C.L.H., J.T.P., C.A.C., R.P.M., K.G., F.P.C., B.H.R., and K.L.S. analyzed data; R.E.S., C.L.H., J.T.P., and R.P.M. performed data collection; and M.M., R.E.S., C.L.H., J.T.P., C.A.C., F.P.C., B.H.R., and K.L.S. wrote the paper.

The authors declare no competing interest.

This article is a PNAS Direct Submission.

[1]To whom correspondence may be addressed. Email: monique@mbari.org.

This article contains supporting information online at https://www.pnas.org/lookup/suppl/doi:10.1073/pnas.2214567120/-/DCSupplemental.

Published March 22, 2023.

Because upwelling may be changing with climate (19, 20), and as artificial upwelling is being considered as a means to increase oceanic productivity (21), elucidating the links between upwelling and ecosystem variability is of great importance.

Here we address two basic questions: 1) Does variation in upwelling drive ecosystem temporal variability from the surface to the deep seafloor? 2) If yes, what are the processes by which this forcing occurs? A previous study has proposed that biological populations "integrate" environmental forcing by damping their response over timescales linked to animal lifespan (22) with subsequent research supporting similar conclusions for plankton (23) and fish (24) populations. Here we examine this hypothesis for surface, midwater, and benthic communities in the California Current using biological time series data. We first characterize the temporal variability of the three communities using principal component analysis (PCA) and then correlate the first principal components to the temporal patterns of upwelling when integrated at different timescales. Finally, we examine hypotheses regarding the mechanisms connecting upwelling to ecosystem variability.

Results and Discussion

Community Variation Over Time: Surface, Midwater, and Benthos. The three time series programs presented here survey plankton biomass using epifluorescence microscopy (surface) and animal density using remotely operated vehicle surveys (midwater and benthos). The resulting time series for surface auto- and heterotrophic plankton (Fig. 1*A*), midwater gelata, micronekton, and macrozooplankton (Fig. 1*B*), and benthic macrofauna (Fig. 1*C*) display considerable variability. Over the past three decades, most taxa fluctuated from very low to very high abundance values (even with extreme values minimized by applying a fourth-root transform), with some taxa exhibiting much higher ranges of variability than others. This result is on par with previously published ecological time series (25) and highlights the complexity of biological systems. Significant intra-community synchrony is visible, defined as most taxa simultaneously increasing or decreasing in density or biomass over time. Oddly, despite this intracommunity synchrony, there is little intercommunity synchrony and the scales of temporal variability differ between the communities. The surface time series

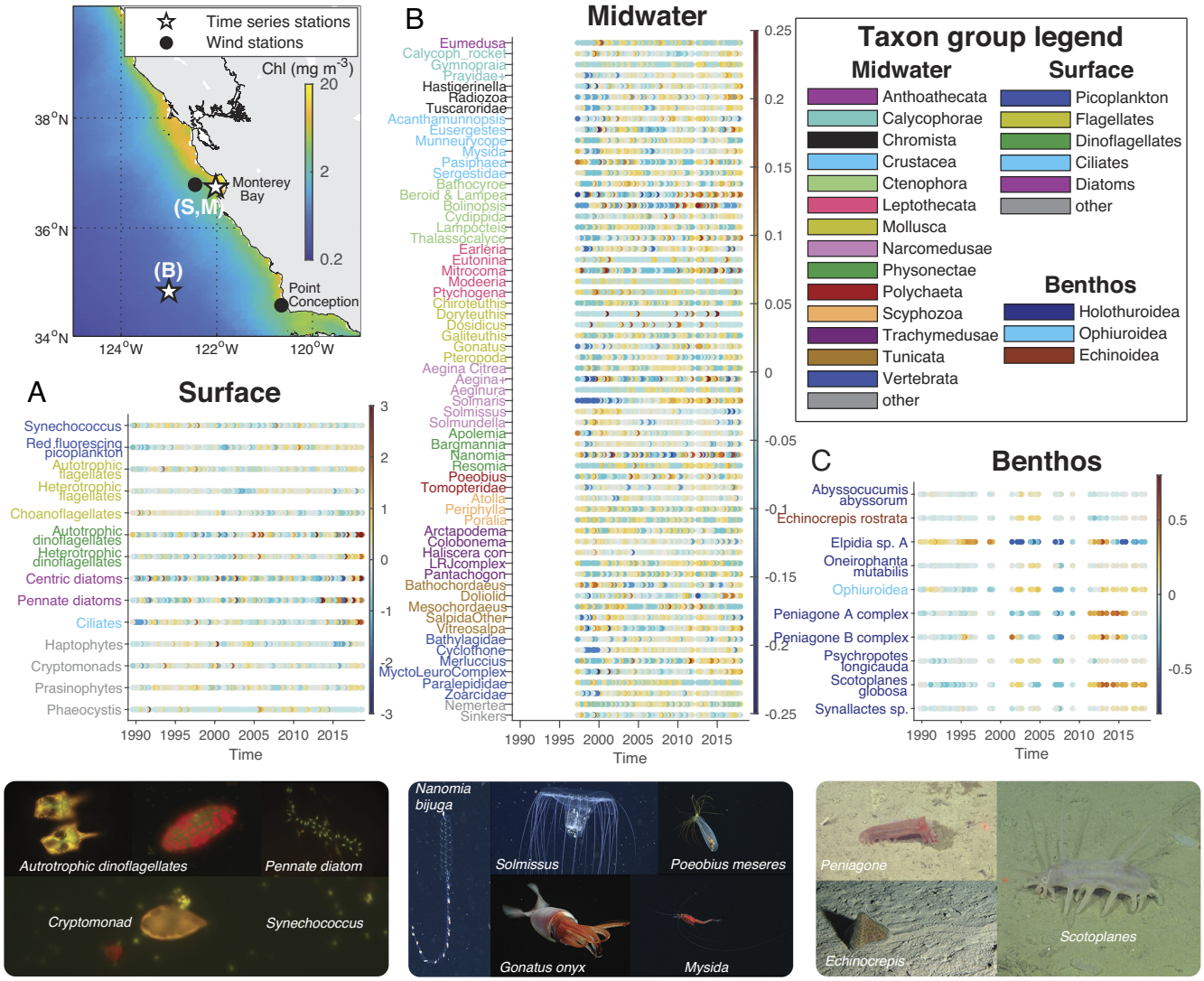

Fig. 1. Presentation of the three time series programs. A map indicates their location (stars; S = surface, M = midwater, B = benthos) as well as wind stations where local upwelling was calculated (Monterey Bay and Point Conception, black dots). Taxon-specific time series are displayed in colors (Fourth-root-transformed and mean removed): (*A*) surface plankton (originally mg m^{-3}), (*B*) 200 to 1,000 m averaged midwater animal density (originally counts per m^3), (*C*) benthic animal density (originally counts per m^2). Taxon names are color-coded according to major groups specific to each time series (see taxon group legend). Photographs of key representative taxa from each time series are shown below each panel. See *SI Appendix*, Fig. S1 for a time-series plot.

alternates very quickly between low and high biomass, while the midwater and benthic communities are characterized by longer periods of positive or negative anomalies. This is not surprising considering that turnover rates of epiplankton are very high while midwater and deep-sea benthic animals often display slow growth and turnover rates (26).

Intracommunity synchrony, likely associated with overall changes in community biomass, abundance, and productivity, is captured by the first mode of variability identified by PCA, termed mode 1 (Fig. 2). For each community, mode 1 is composed of a time series (first principal component, hereafter PC1) and of taxon-specific loadings indicating how strongly each taxon is associated with PC1, with the highest loadings identifying taxa accounting for the most variation along the PC1 axis. Within each of the three communities, most loadings are of the same sign; loadings of opposite signs are small and few. In other words, mode 1 represents synchronous changes in biomass or density across taxa rather than changes in community structure. Surface PC1 is indeed strongly correlated with total plankton biomass (r = 0.67, $P << 0.01$), as well as independent in situ measurements of vertically integrated chlorophyll (r = 0.69, $P << 0.01$) and primary production (r = 0.55, $P << 0.01$). While surface PC1 is highly seasonal, these correlations hold after removing a monthly seasonal cycle (r = 0.63 and 0.44 for integrated chlorophyll and primary production, respectively, $P << 0.01$). Midwater and benthic community measurements did not include biomass or productivity; however, the PC1s are correlated with total animal density (r = 0.74 and r = 0.79, respectively, $P << 0.01$).

While mode 1 similarly captures, for all communities, overall changes in taxa density and/or biomass, the corresponding temporal patterns (PC1s) are very different between the surface, midwater, and benthic communities (Fig. 2 and *SI Appendix*, Table S1). The strongest variation in the surface community is linked to short-lived phytoplankton blooms that occur seasonally, although interannual variability is also present (Fig. 2*A*). Seasonal variations are also visible for the midwater, but midwater and benthic PC1 mostly display interannual or longer variations. The midwater community displayed unusually low density in 1998 to 1999 and 2005 to 2006, and high density after the late 2000s (Fig. 2*B*). Similar results were obtained for a 23-y annual survey of pelagic nekton and crustaceans in a larger region between Monterey Bay and Point Reyes (27), with the first mode capturing community decreases in abundance in the late 1990s and mid-2000s. For the benthos, very high animal densities were observed between 2012 and 2014, very low around 2007, and average densities at other times (Fig. 2*C*).

Integrated Upwelling Explains Surface-to-Seafloor Ecosystem Temporal Variability. We investigated the link between upwelling and ecosystem variability by calculating correlations between PC1s and a range of cumulative integrations of the upwelling signal (22, see *Materials and Methods*). Integrations are mathematically similar to exponential moving averages and represent the superimposed effect of past upwelling conditions, with recent events having more weight than past ones, effectively producing signals characterized by increasing low-frequency variability as integration timescales increase (22). For a given community, the best-fitting integration timescale (for which the maximum correlation is obtained) identifies the community's intrinsic damping timescale, a biological characteristic representing the timescale over which the community responds to upwelling.

The upwelling integration curve (correlation as a function of integration timescale) is different for each community (Fig. 3*A*). The correlations peak quickly for the surface community, suggesting an intrinsic damping timescale of 16 d, and then decrease. Integration of upwelling at this 2-wk timescale creates a strongly seasonal signal

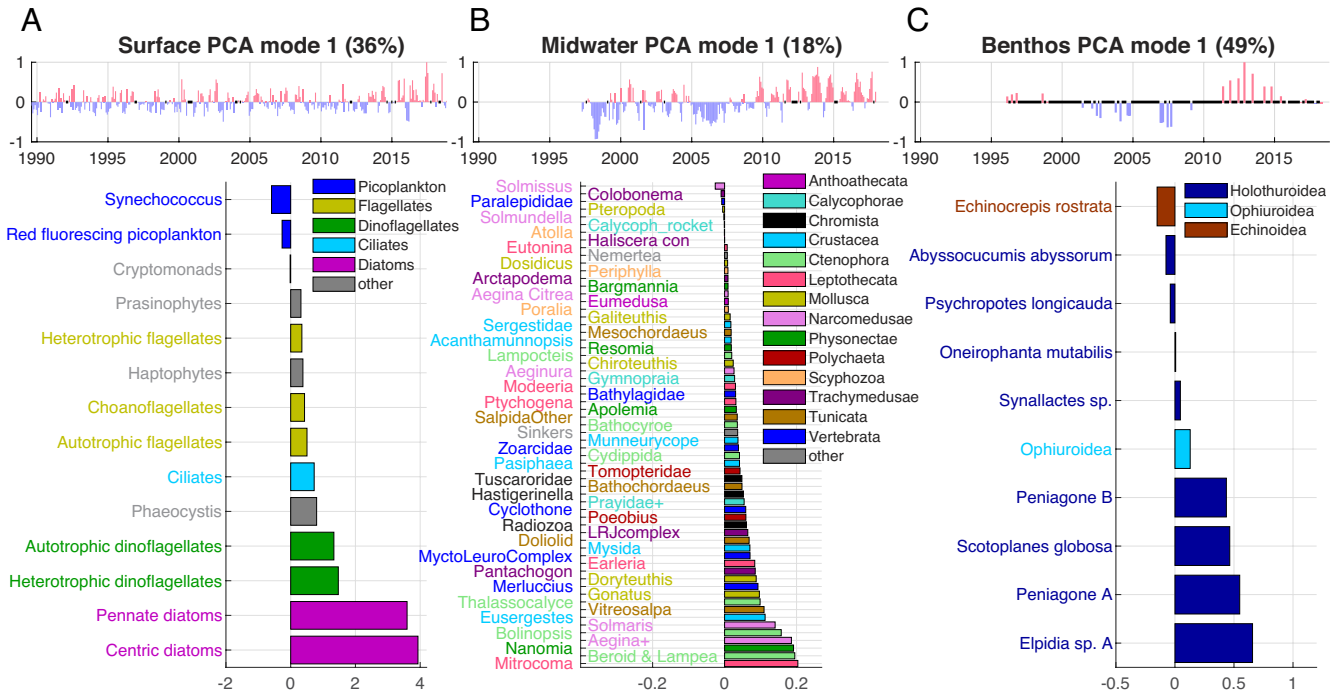

Fig. 2. First PCA mode for the three communities: (*A*) surface, (*B*) midwater, and (*C*) benthos. For each community, the *Top* panel displays the principal component (PC1), averaged monthly with 1-mo gaps filled by linear interpolation for better visualization (remaining gaps are indicated in black). The *Bottom* panel displays the taxon-specific loadings, sorted graphically so that taxa scoring similarly on a given mode are displayed next to each other. For each community, this mode shows most taxa increasing and decreasing over time with little change in community structure, although the temporal variability differs between the three communities. Due to space constraints, midwater taxon names are displayed in two columns. The benthic time series had to be shortened to obtain a first PCA mode statistically separable from the second (*Materials and Methods*). The colors correspond to taxonomic groups specific to each time series.

correlated with the surface community (Fig. 3*C*). For the benthos, correlations increase with integration timescales, remaining high with timescales above 3 y and peaking at 4.5 y. Finally, for midwater, the integration curve is asymptotic so that no intrinsic damping timescale was defined, although the most significant correlation was obtained for a damping timescale of 1.2 y (*SI Appendix*, Fig. S2).

The correlations between integrated upwelling and the three PC1s suggest that periods of high upwelling favor increases in organism biomass or density throughout the water column. However, the different integration curves and damping timescales indicate that each community responds to upwelling over different timescales, explaining the lack of intercommunity synchrony. Spatial variations

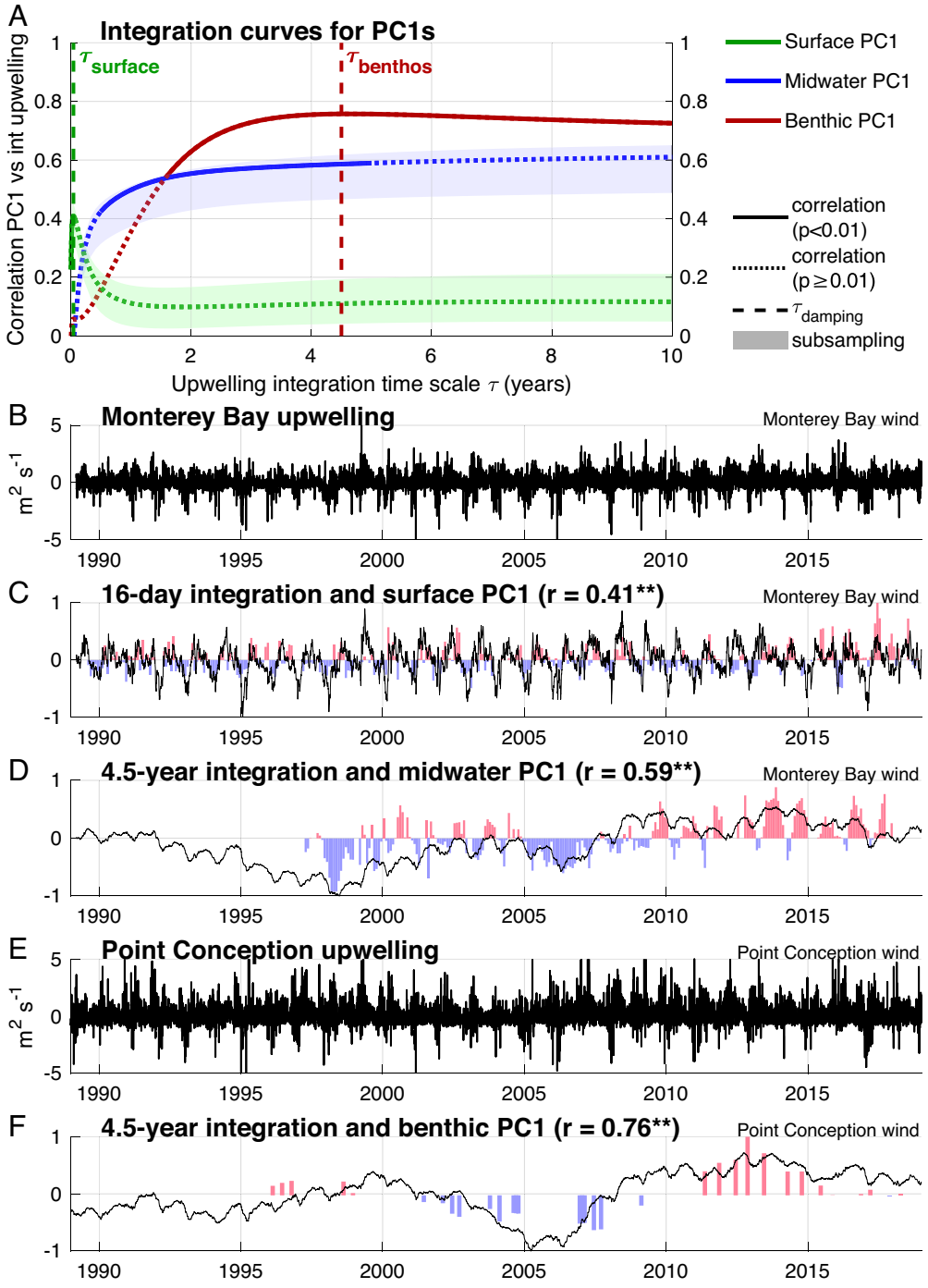

Fig. 3. Relationship between integrated upwelling and PC1 for the three communities. (*A*) Integration curves: correlation coefficients between each PC1 and integrated upwelling for a range of integration timescales. Correlations for which $P \geq 0.01$ (adjusted for autocorrelation) are indicated with dots; the *P* values are displayed in *SI Appendix*, Fig. S2. The high correlations suggest that periods of high upwelling favor increases in organism biomass or density, although each community responds over different timescales. The damping timescale (maximum correlation, vertical dashed lines) is 16 d for the surface, 4.5 y for the benthos, and undefined for midwater. Shaded areas highlight the spread of correlation (width one SD, centered around the mean) when considering 500 randomly subsampled datasets for surface and midwater based on benthos temporal resolution. (*B*) Original upwelling time series for Monterey Bay (no integration). (*C* and *D*) Monthly PC1 for the surface and midwater communities as in Fig. 2 (shaded blue/pink) and daily Monterey Bay upwelling integrated using different timescales, normalized to PC1 (black lines). (*E*) Same as (*B*) for the Point Conception upwelling. (*F*) Same as (*C*) and (*D*) for the benthic community using Point Conception upwelling. Correlation coefficients ($P < 0.01$, adjusted for autocorrelation) were computed between PC1 (original temporal resolution) and integrated upwelling time series on coincident daily time steps, except for the benthos where monthly averages were used. The same correlations with nonintegrated upwelling are: surface r = 0.24, midwater r = −0.18, benthos r = −0.04.

in upwelling may play a role too. Given their ~230 km geographic separation, the midwater and benthic communities were compared to different upwelling time series (Monterey Bay and Point Conception, respectively). Interestingly, the 4.5-y–integrated upwelling time series are fairly different between Monterey Bay and Point Conception (Fig. 3 *D* and *F*), and the midwater and benthic communities are each strongly correlated with their local upwelling time series but less so with the time series from the more distant site (particularly for the benthos, *SI Appendix*, Table S2). This suggests that site-specific upwelling patterns are important and may explain spatial differences in ecosystem temporal variability.

What explains the correlation between integrated upwelling and ecosystem variability, as well as the different integration curves and damping timescales identified for each community? The link between integrated upwelling and the three PC1s can be explored through two hypotheses (Fig. 4): [H1] Communities respond to wind-driven coastal upwelling although their damping timescales are different (hereafter direct link), and/or [H2] Communities vary in response to other oceanic variability that is synchronous with integrated upwelling (hereafter indirect link). Under H1, the communities respond to previous and current upwelling-induced nutrient supply as the responses persist, overlap, and fade over some period of time, resulting in a damped and prolonged biological response. The connection between nutrient supply and the three communities would occur via changes in primary production, vertical carbon flux, and more generally food source for midwater and benthic communities. Indeed, despite its strong seasonal variability, the surface community also includes an interannual component correlated with integrated upwelling that could propagate to deeper communities. Under H2, the biological communities do not integrate the upwelling forcing directly. Instead, they respond to some other forcing whose low-frequency variability is similar to the upwelling low-frequency variability emphasized by the integration calculation. Such forcing may include oceanic circulation, local conditions such as temperature or oxygen concentration, and remote conditions such as source water characteristics. These two hypotheses are not exclusive and under both, climate variability impacts biological communities, either via upwelling or via other oceanic forcing correlated with upwelling.

Direct and Indirect Connections Between Upwelling and Biological Communities. A direct causal link between upwelling and ecosystem variability (H1) appears most likely for the surface and benthic communities. While correlations between surface PC1 and 2-wk integrated upwelling are mostly driven by similar seasonal cycles, 2-wk integrated upwelling is also strongly correlated with chlorophyll and primary production, which are more direct measures of the phytoplankton community productivity, at all timescales including interannual and longer (*SI Appendix*, Table S3). These strong correlations occur because upwelling supplies nutrients, directly supporting primary production. Wind-driven nutrient supply is the strongest driver of primary production at the seasonal scale off California (14), and can similarly be expected to drive interannual variability in primary production. Supposing a tight coupling between auto- and heterotrophic plankton, a direct link between upwelling and the entire surface planktonic community from months to decades is very likely (15). At 4,000 m, the physical environment (e.g., local temperature) is relatively stable, but considerable variability in the benthic community nevertheless occurs and has been shown to correlate with climate fluctuations (28, 29). Significant increases in animal abundance and reproductive activity have followed large depositions of fresh phytodetritus,

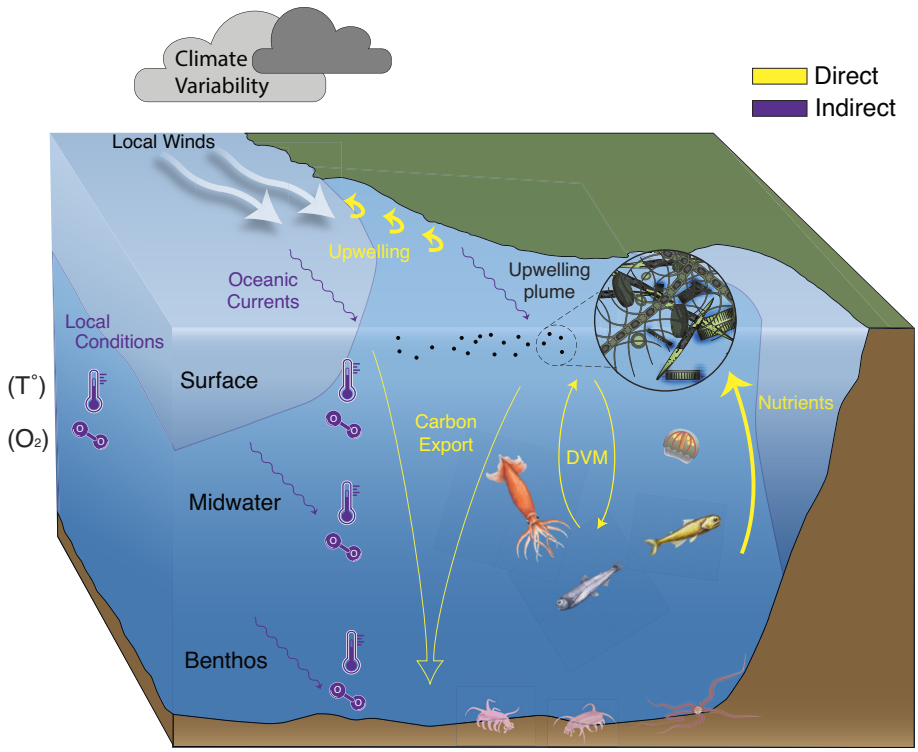

Fig. 4. Direct and indirect processes connecting wind forcing to biological communities through the water column. Large-scale and local climate variability impact local winds and environmental conditions such as oceanic currents, temperature, oxygen concentrations, and nutrient concentration at depth. As such, atmospheric forcing is connected to biological communities both directly (via changes in wind-driven nutrient supply) and indirectly (via changes in local environmental conditions). Upwelling, driven by local winds, brings nutrients to the sunlit waters sustaining phytoplankton. Midwater animals are connected to surface biological communities via feeding in surface waters at night during diel vertical migration (DVM), and via the vertical export of surface organic matter to depth (carbon export). A portion of carbon export ultimately sinks to the seafloor, sustaining benthic communities. The surface, midwater, and benthic communities each integrate the upwelling forcing but do so at different frequencies (damping timescales), resulting in different temporal variation (Fig. 3).

fecal pellets, and carcasses of salps, all of which are derived from surface phytoplankton or its grazers (30, 31). Carbon export to depth measured from sediment traps is correlated with upwelling (32) and time lags between changes in satellite-derived estimates of surface export flux and benthic processes are relatively short (<70 d, ref. 33) so a direct connection to upwelling is highly plausible, although it does not explain the 4.5-y damping timescale.

The link with upwelling is more difficult to establish for the midwater community, as the drivers of change in midwater animal density in Monterey Bay are less clear. Two major processes can be considered: 1) changes in the food source, which is mostly surface production consumed by primary consumers then exported to the midwater via feeding interactions, diel vertical migration (DVM), and sinking detritus (34); or 2) oceanic currents, which may advect communities in a way that modifies animal density if midwater animal density is geographically heterogeneous. The former implies a link with upwelling-driven primary production (thus related to H1) while the latter implies a link with oceanic variability potentially correlated with integrated upwelling (thus related to H2). As depicted by PC1, the midwater community mostly varies at interannual to decadal timescales. At those scales, midwater PC1 is strongly correlated with other environmental predictors with lags up to 1 y, such as alongshore advection and the North Pacific Gyre Oscillation (NPGO), a low-frequency climate mode that impacts oceanic currents, nutrients, and oxygen (35) (*SI Appendix*, Fig. S3). Ecosystem variability in the region has been previously linked to large-scale climate phenomena (36–38), and NPGO-driven changes in gyre circulation and source waters may impact midwater communities as surveyed at a fixed station. The NPGO reflects changes in upwelling strength off central and southern California (35), so the correlation between midwater PC1 and integrated upwelling could be a result of both being driven by the NPGO (H2), although the 1-y lag remains unexplained.

In addition to potential influences of advective processes on the midwater community (H2), several facts support a direct integration of the upwelling signal via primary production (H1). First, the midwater PC1 is correlated with integrated surface primary production (r = 0.48 with a 4.5-y integration on monthly time series, $P = 0.09$). Second, contrary to advection-related predictors, integrated upwelling is best correlated with midwater PC1 at zero lag, for which it displays the highest correlation of all predictors (*SI Appendix*, Fig. S3). The correlations are stronger when upwelling is integrated rather than low pass-filtered, suggesting that the midwater community is more likely to integrate upwelling than to be driven by its low-frequency variability (22). Most importantly, the relationship between midwater PC1 and integrated upwelling masks differences across taxa. While midwater taxa densities are significantly correlated ($P < 0.05$) with integrated upwelling for 38% of the taxa, the taxon-specific correlations peak at different damping timescales (Fig. 5 and *SI Appendix*, Table S4) that tend to increase with depth (*SI Appendix*, Fig. S4). If the midwater community did not integrate upwelling but was mostly responding to low-frequency environmental variability such as the NPGO, then all taxa should correlate similarly with upwelling as it relates to the NPGO. Instead, taxon-specific damping timescales suggest that the different midwater taxa directly integrate upwelling variability over distinct timescales. The diversity of the midwater community being surveyed (63 taxa), combined with taxon-specific damping timescales and temporal variability, likely explains both the relatively small percentage of variability captured by mode 1 (18%, Fig. 2) and the lack of a well-defined damping timescale at the community level (Fig. 3*A*). By contrast, taxa included in the surface and benthic PCA analyses are fewer, less phylogenetically diverse, and display relatively similar damping timescales (*SI Appendix*, Table S5). We also note that two possible paths had been proposed for integration of atmospheric forcing (22): a single integration path via changes in productivity and a double integration path via changes in horizontal transport. Our results suggest that a single integration can be sufficient to explain the temporal variability of surface, midwater, and benthic communities (Fig. 3) as well as individual taxa (Fig. 5).

Biological Damping Timescales. Assuming that all three communities integrate the upwelling forcing via primary production and trophic transfer (H1), what constrains the observed damping timescales? The species that compose the surface plankton community are characterized by fast growth rates and rapid turnover and thus respond quickly to environmental forcing (39, 40). The observed 2-wk damping timescale matches the time needed to consume upwelled nutrients (41) and the timing of phytoplankton response to upwelling in a model (42). Faster-growing midwater animals may track detrital concentrations at depth at similar short timescales. However, for most midwater and benthic animals, longer and taxon-specific damping timescales suggest that forcing and response become decoupled due to a biological memory effect linked to life history traits. One hypothesis would be cohort resonance (43), a process by which populations are more sensitive to some frequencies of environmental variability, and notably to periods corresponding to the dominant age of spawning (44). This hypothesis is countered by the fact that most taxa are better represented by an integration (which does not select specific frequencies) than by a low-pass filter of upwelling. Trophic transfers and predator-prey interactions may also damp upwelling forcing to some extent (23, 24), as a wind-driven increase in primary production will take some time to propagate through the food web and may be successively integrated by each trophic level. Yet, trophic damping seems unlikely to explain timescales of several years. Trophic transfer times for carbon were found to be less than a month per trophic level in another upwelling ecosystem (45) and it is generally believed that upwelling food webs are relatively short, at least in the upper ocean (46, 47). We note, however, that the deep pelagic food web is complicated by feeding interactions within the "jelly web" (34), with circular rather than linear transfers. These can act to increase trophic damping as nutrients have the potential to recirculate multiple times through a given trophic group.

As originally proposed by Di Lorenzo and Ohman (22), damping of the upwelling forcing is likely related to the lifespans of organisms within a biological community. Under this hypothesis, an upwelling-driven increase in animal numbers would persist until the animals die; animal abundance at any given time would then reflect both lifespan and the history of upwelling events. To test this idea, we used a simple age-structured model forced by upwelling to assess the impact of lifespan on the population dynamics of individual taxa (see *Materials and Methods* and *SI Appendix*, Fig. S5). Different lifespan parameterizations were tested and the time series produced by the model were compared to time series of individual midwater and benthic taxa (e.g., Fig. 5 *A* and *B*). For a given taxon, the best model parameterization was chosen as the most successful in reproducing a taxon's temporal variability. The corresponding output not only correctly reproduced the taxon time series but, also, its upwelling integration curve matched the shape of the taxon's integration curve. As a consequence, the damping timescale of the modeled time series was similar to the taxon's (Fig. 5 *C* and *D*). For all the parameterizations, modeled damping timescales were close to the mean lifespan in the model (Fig. 5*E*). When matching each taxon to its best parameterization, observed taxon-specific damping timescales were also similar to the mean lifespan in the model (Fig. 5*F*). Taken together,

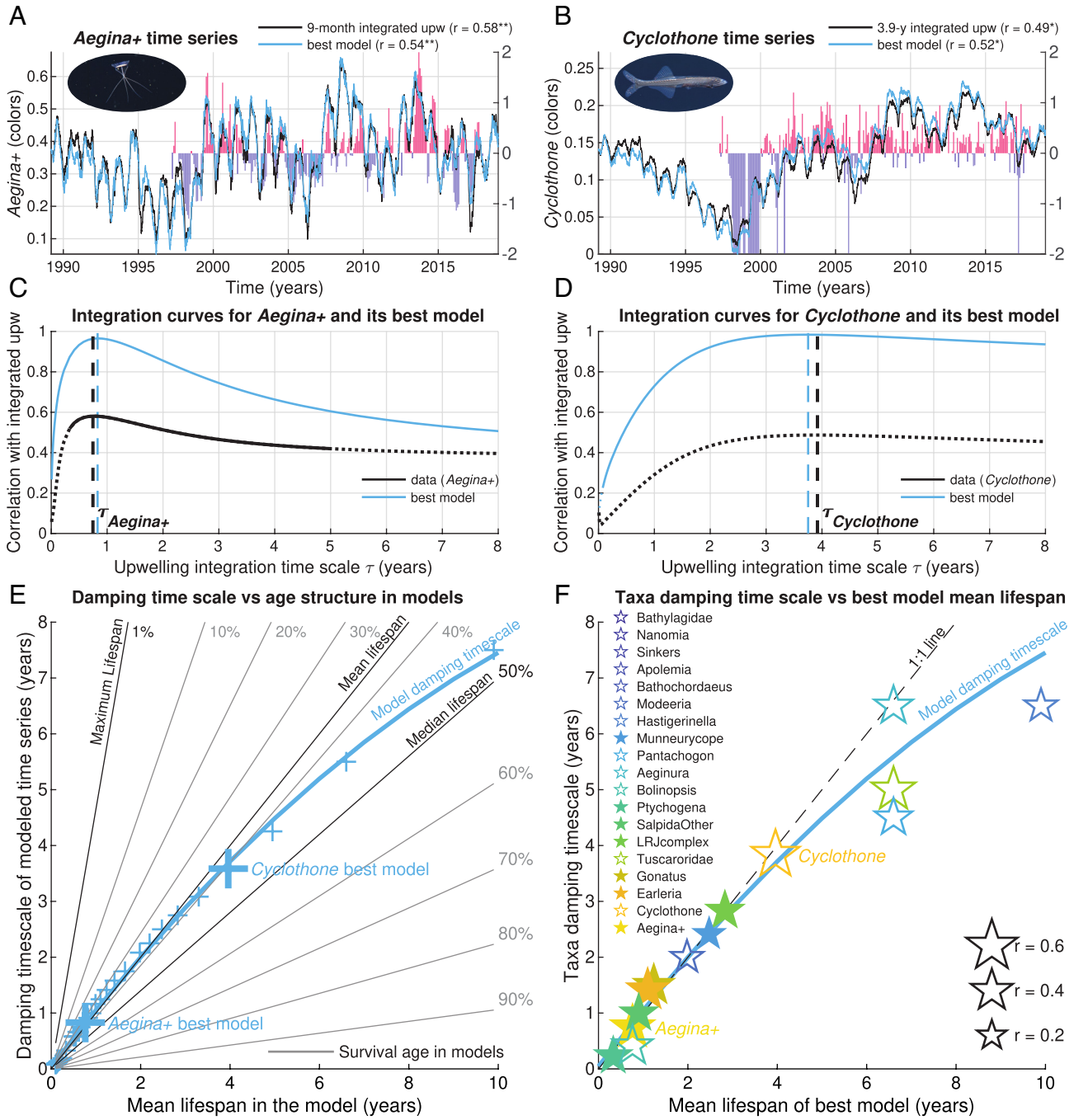

Fig. 5. Relationship between taxon-specific time series, integrated upwelling, and age structure. (*A*) Comparisons between observed taxon density (colors), Monterey Bay integrated upwelling (black), and output from an age-structured model (blue) for the medusa group *Aegina*+ (includes several species of *Aegina*-like narcomedusae). Observed density was fourth-root-transformed and averaged monthly with 1-mo gaps filled as in Fig. 2. Upwelling was integrated using the *Aegina*+ damping timescale of 9 mo. The model parameterization best representing *Aegina*+ (characterized by a natural mortality rate of 1.3 y^{-1}) was used. (*B*) Similar to (*A*) but for the fish *Cyclothone* instead of *Aegina*+. The model parameterization best representing the *Cyclothone* time series was characterized by a natural mortality rate of 0.25 y^{-1}. In (*A*) and (*B*) legends, significance levels are indicated as ** ($P < 0.01$) or * ($P < 0.05$). (*C*) Integration curves for *Aegina*+ (black) and the model output (blue, computed over the 1989 to 2018 time period). Dashed lines indicate the damping timescale (best-fitting integration timescale) for the data and model time series. Even though correlation strength differs, the shape of the two integration curves is similar, indicating that age structure (as implemented in the model) is sufficient to explain the relationship with integrated upwelling and is likely to drive the damping timescale. (*D*) Similar to (*C*) but for the fish Cyclothone instead of Aegina+. In (*C*) and (*D*), correlations for which $P \geq 0.01$ are dotted (P remains <0.05 for Cyclothone). Taken together, these four panels show that Cyclothone and *Aegina*+ both are correlated with integrated upwelling but their temporal variability, best model parameterization, and integration curves are very different. (*E*) Blue: relationship between damping timescale and mean lifespan across the different model parameterizations ("+" = each parameterization, line = second-order polynomial fit). For a given parameterization, the damping timescale of modeled time series is the best-fitting integration timescale when comparing integrated upwelling (forcing the model) and the model output [e.g., dashed blue lines in panels (*C*) and (*D*)]. Bold highlights the best parameterization identified for *Aegina*+ and Cyclothone. Grey/black lines indicate the age at which a given percentage of the population survived, from 100% (at age 0) to 1% (maximum lifespan in the model). The damping timescale ("+" for each parameterization) falls between the mean (1:1 line) and median lifespans. (*F*) Relationship between individual midwater taxa damping timescales when identified (bold numbers in *SI Appendix*, Table S4; dashed black lines in panels *C* and *D* for *Aegina*+ and Cyclothone) and the mean lifespan characterizing the model output best correlated with the taxon time series (i.e., same x-value as in panel (*E*). Taxa are sorted according to the correlation between each taxon time series and its associated model output, also represented by the size of the stars. Filled stars indicate $P < 0.01$; open when $P < 0.05$ (not displayed otherwise).

these results support the idea that the intrinsic damping timescale of individual taxa as well as biological communities are related to organism lifespans, explaining how different taxa and communities can respond to the same upwelling time series with very different temporal variabilities (Figs. 3 and 5).

Integration curves and damping timescales could thus provide a framework for estimating how long some of the midwater and benthic animals live, or more accurately, the portion of their life cycle that is sampled by the time series (Fig. 5 *E* and *F* and *SI Appendix*, Tables S4 and S5). This aspect is as difficult to validate as it is important, because methods for assessing lifespans are currently lacking for the majority of deep-sea taxa. Lifespan has been assessed for relatively few deep-living organisms, many of them fishes (48), some cephalopods (26), and crustaceans (49), using mark-recapture techniques or growth rings in hard structures. Having a variety of ways to estimate lifespan would be extremely beneficial, especially as climate change alters marine phenology and the reliability of age estimates based on growth rings (50). We emphasize that using damping timescales as an indicator of typical lifespan is a hypothesis that requires validation, but it fits with the long-standing paradigm that longevity is correlated positively with depth (*SI Appendix*, Fig. S4) (26, 51). Where lifespan data exist, we provide comparisons to the damping timescale to support our results (*SI Appendix*, Table S4).

Conclusions

The first mode of variability in surface, midwater, and benthic communities captures synchronous fluctuations in plankton biomass (surface) or animal density (midwater and benthos) across most taxa within each community. For the three communities, changes in overall biomass or abundance thus explain the most variance in the time series, rather than changes in species composition and community structure. This temporal variability is not synchronous across communities, but each community PC1 is nevertheless correlated with local upwelling variability integrated at different timescales. The result suggests that upwelling drives surface-to-seafloor ecosystem variability in the California Current system, explaining 17% of the variability in surface PC1, 34% for the midwater, and 58% for the benthos (Fig. 3). Both direct (via primary production) and indirect (via coincident ocean changes) processes appear to contribute to these correlations. We propose that the dominant process is a direct connection between upwelling and the biological communities, where upwelling is damped at timescales linked to how long upwelling-driven changes persist within each community. These damping timescales appear related to organism lifespan which may increase from surface to depth. Identifying animals' damping timescales from integration curves (Figs. 3 and 5) can thus provide clues about typical lifespan for animals in the ocean. While this aspect requires validation, our estimates of taxon-specific damping timescales have a strong potential for assessing typical lifespans, particularly in the deep ocean where lifespans remain largely unknown.

Materials and Methods

Surface Time Series. Plankton biomass was estimated from surface plankton counts collected using ship-based CTD-rosette at station M1 in Monterey Bay (122.022°W, 36.747°N). This station is part of a three-station time series program operating in Monterey Bay since 1989 at 3 to 4-wk intervals (7). Epifluorescence microscopy was used to enumerate and size auto- and heterotrophic plankton. Starting in 1998, flow cytometry samples provided more precise numbers for *Synechococcus* and eukaryotic picoplankton (*Prochlorococcus* was not included as no information is available prior to 1998). Standard geometric equations (e.g., ellipsoid, sphere, cylinder, pennate diatom shape) were used to calculate biovolumes of individual cells, and biomass of each plankton group was assessed using biovolume-based carbon conversions. For picoplankton an average value per cell was used (52): 82 fgC cell^{-1} for *Synechococcus* and 530 fgC cell^{-1} for eukaryotic picophytoplankton (red fluorescing picoplankton). Diatom biovolumes were converted to biomass using $\log_{10}(\text{Biomass}) = 0.76\ \log_{10}(\text{Volume}) - 0.29$ where Biomass is in gC and Volume is in μm^3 (53). The ciliate conversion was Biomass = 0.08 * Volume (54). For all other plankton, we used $\log_{10}(\text{Biomass}) = 0.94\ \log_{10}(\text{Volume}) - 0.6$ (53).

Midwater Time Series. Quantitative mesopelagic video transects were conducted at a single station in Monterey Bay (Midwater 1, 36°42′N, 122°02′W) (8). The station is located over the axis of the Monterey Submarine Canyon, where the water column is approximately 1,600 m deep. Data were collected using remotely operated vehicles (ROVs). Estimates of animal densities using ROV imaging underestimate some groups (notably fishes), but provide a more complete view of life in the ocean than traditional methods such as nets and acoustics, particularly for gelatinous animals (8). The ROVs conducted horizontal video transects while moving at about 0.5 m s^{-1} for 10 min. Data for this paper come from approximately monthly transects made at 100-m intervals between 200 to 1,000 m from 1997 to 2017. These years were chosen because the entire mesopelagic water column was more evenly surveyed than in the years prior. In each transect, the community of animals was annotated by professional annotators using the open-source Video Annotation and Referencing System (VARS) software (55). Annotators identified organisms in transect video to the lowest taxon possible; in many cases to species. We selected 63 taxonomic groups defined at the highest possible taxonomic resolution (*SI Appendix*, *Text* S1 and Table S6); annotations not included represent 31% of the total (84% of which are euphausiids, chaetognaths, and unidentified appendicularians). Calibrated cameras on ROVs and accurate measurement of ROV speed through water, allow for the calculation of volume for each transect. Animal density was calculated for each taxonomic group and each depth-specific transect as the number of individuals divided by the corresponding transect volume, further averaged over the water column from 200 to 1,000 m. Midwater transecting methods and their efficacy are well-documented (56, 57).

Benthic Time Series. Two comparable methods were used to assess benthic communities at Station M (34°50′N, 123°00′W) (9). From 1989 to 2005, the identification of the lowest possible taxon, and quantity of benthic animals were recorded from images taken by a camera-sled towed along a horizontal transect above the sea floor at a speed of approximately 1 m s^{-1}, taking a film image every 4 to 5 s (water depth ~4,100 m). The developed film was projected by a Beseler model 23C-II enlarger for the annotation of identifiable animals in images (58). Further details can be found in ref. 59. From 2006 to 2018, benthic communities were assessed using ROV video transects recorded from approximately 1.3 m above the sea floor, with a view of approximately 1 m wide, and length typically approximately 1 km. Water depth for these transects was approximately 4,000 m, the lower depth limit of the ROV. Animals visible in the video were identified and annotated using VARS. The 2006 change in sampling method and in time series location and depth was investigated by ref. 60 and found to have little impact on the megafauna time series. Further details can be found in ref. 29.

Principal Component Analysis. In order to synthesize the information provided by dozens of individual taxa into a single time series that explains most of the variance in the dataset, the three communities were separately analyzed by PCA. Prior to analysis, data were transformed using a fourth root, and the mean of each taxon-specific time series was removed. No trend or seasonal cycle was removed. Even with the fourth-root transform, most weight is on abundant species. All resulting first PCA modes were checked for statistical separation from the second mode following North's rule of thumb (61). The benthic PCA failed this test and early dates from the benthic time series were iteratively removed until the resulting PCA passed the test, which was obtained by removing the years 1989 to 1995. Furthermore, a couple of potential biases for the benthic PCA were examined. First, temporal resolution is much lower for the benthos (on average 1.4 survey/year) than for the surface (14.1 survey/year) and midwater (9.8 survey/year) time series. To account for this difference, PCA was also run on 500 randomly selected midwater and surface surveys, corresponding to the benthos sampling frequency (41 out of 413 surface surveys for 1989 to 2018, and 29 out of 203 midwater surveys for 1997 to 2017). An additional constraint was that at least

one survey was selected each year to ensure consistent coverage over time. The resulting 500 first principal components were used to assess the sensitivity of the results to temporal resolution (Fig. 3*A*). A second potential bias exists in that the benthic variability was based on only 10 echinoderm species, while surface and midwater communities were more extensively surveyed. Surveys of the full benthic community (107 taxa) are available starting in 2007 with ROV video. The ROV and echinoderm time series were similarly analyzed using PCA over the ROV time period and found to yield very similar first modes (*SI Appendix*, Fig. S6), suggesting that the benthic PC1 based on 10 echinoderm species likely correctly represents the temporal variability of the full benthic community.

Upwelling. Wind-driven upwelling was computed from hourly winds measured at National Data Buoy Center buoys 46042 off Monterey Bay (1989 to 2018, used for comparison with surface and midwater time series) and PTGC1 near Point Conception (1986 to 2018, used for comparison with the benthic time series), downloaded from https://www.ndbc.noaa.gov. Upwelling (Ekman transport) was computed from alongshore wind stress estimated from wind speed (62) and averaged daily. The 46042 time series had 7.6% missing time steps with gaps up to a year that were filled using a nearby mooring (M1, operated by the Monterey Bay Aquarium Research Institute) using a linear regression between upwelling time series at both moorings ($r = 0.83$, $P << 0.01$); the remaining gaps were filled linearly (maximum gap length: 3 d). The PTGC1 time series had 3.8% missing time steps that were similarly filled using the 46042 buoy ($r = 0.68$, $P << 0.01$); the remaining gaps were filled linearly (maximum gap length: 19 d).

Integration and Damping timescale. Integration was computed iteratively as $dF/dt = f(t) - F(t)/\tau$ (22), where f is the forcing time series (upwelling, mean removed), τ a prescribed integration timescale, and F the resulting integrated time series. F was normalized to the SD of the forcing time series f. Mathematically, F at a given time is a weighted average of past f values (past upwelling events), those values decreasing in importance exponentially with time. The speed of this decrease with time is controlled by the integration timescale τ. Integrated time series were correlated with biological time series over a range of τ ("integration curve", e.g., Figs. 3*A* and 5 *C* and *D*). Pearson correlation coefficients were calculated between the biological time series and the daily integrated upwelling time series subsampled on the same days. This means correlations were calculated on a daily basis even though only a small percentage of days are available. The integration timescale τ that generates the highest correlation between integrated forcing and the time series of a given biological variable (e.g., community PC1 or taxon time series) represents the intrinsic damping timescale of that variable for the forcing f (here upwelling). Because integration is based on past forcing values, the earliest part (order of τ) of the integrated time series F is subject to caution since past values are unknown, and could therefore bias the damping timescale detection. However, the surface community has a short damping timescale and the midwater time series starts 9 y after its upwelling time series starts, so surface and midwater results are unlikely to be impacted (integration curves were constructed for τ up to 10 y). The benthic PC1 starts in 1996 (see above) 10 y after upwelling so the benthos damping timescale identified from PCA is not impacted.

Significance Levels. Throughout the paper, the significance of Pearson correlations between time series (including in integration curves) was assessed using *P* values calculated using the modified Chelton method recommended by ref. 63 to account for autocorrelation in the time series. The method requires regular time steps, so *P*-values were assessed using biological time series averaged monthly with 1-mo gaps filled by linear interpolation (daily integrated upwelling was averaged monthly postintegration). Significance levels for benthic time series are subject to caution due to numerous gaps in monthly time series. The integration curves are very similar when computed on a daily (Fig. 3*A*) or monthly (*SI Appendix*, Fig. S2*A*) basis. Because integrated upwelling autocorrelation increases with increasing τ, the highest correlation (observed when τ is equal to the damping timescale) does not necessarily coincide with the most significant correlation in integration curves (*SI Appendix*, Fig. S2). Throughout the paper, $P < 0.01$ is indicated by **, $P < 0.05$ by *, and $P \geq 0.1$ by n.s. (non-significant).

Population Modeling. An age-structured model, in which the density of newborn animals is proportional to positive upwelling, was used to test whether a biological integration could explain the observed damping timescale for a given taxon. The model was similar to age-structured models used for fish populations (64) and represents animal density within daily-resolved age groups function of time and age, with the total population being the sum of all age groups. At each time step (resolution dt = 1 d), animals transfer from one age group to an older one, except for a portion that dies. Individuals entering the population (age 0) are proportional to daily, positive upwelling. The equations giving taxon density as a function of time and age are:

$$\mathrm{ModelTaxa}(t, \mathrm{age} = 0) = \max(0,\ \mathrm{upwelling}(t)),$$

$$\mathrm{ModelTaxa}(t, \mathrm{age} \geq 1) = \mathrm{ModelTaxa}(t-1, \mathrm{age}-1) * e^{-m*dt},$$

where m is the natural mortality rate, constraining the modeled age pyramid. In the model, the maximum lifespan was defined as the age where animal density drops below 1% of density at birth, and the mean lifespan (life expectancy at birth) was calculated from the age pyramid. In total, 32 versions of the model were built (for m ranging from 0.1 y^{-1} to 10 y^{-1}), and forced by daily upwelling. The resulting modeled time series ModelTaxa were correlated with measured taxon-specific midwater and benthic time series (using the same fourth-root transform as used for in situ data). The parameterization corresponding to the highest correlation provides information on potential biological parameters of the taxa being considered. See *SI Appendix*, Fig. S5 for an example.

Data, Materials, and Software Availability. The three time series were deposited in Zenodo (65). The code to reproduce figures and main results from the paper was deposited in Zenodo (66) and is available at https://github.com/messiem/sourcecode_ITS.

ACKNOWLEDGMENTS. We rely on and are grateful for the Monterey Bay Aquarium Research Institute (MBARI) ships, crews, and pilots we have worked with over the years. Engineers A. Sherman, P. McGill, B. Schlining, B. Hobson, and M. Chaffey contributed significantly to the time-series programs at MBARI as has Kim Reisenbichler. This research is possible through the continued support of MBARI management, the MBARI Video Lab, particularly L. Kuhnz, K. Schlining, K. Walz, and S. von Thun, the Video Annotation and Referencing System (VARS), and the David and Lucile Packard Foundation from which our funding comes. The establishment and early monitoring program at Station M were supported by NSF to K.L.S. at Scripps Institution of Oceanography (SIO). We thank the SIO ship's crews, technicians, and engineers, who made Station M successful. We also thank Melissa Mendoza for her work on Figs. 1, 4, and 5, and Zed Ziccarelli for providing plankton images in Fig. 1. Finally, we wish to thank the anonymous reviewers for their constructive comments and helpful suggestions that improved the paper.

Author affiliations: [a]Monterey Bay Aquarium Research Institute, Moss Landing, CA 95039; and [b]Integrative Oceanography Division, Scripps Institution of Oceanography, University of California San Diego, San Diego, CA 92093

1. S. C. Doney *et al.*, Climate change impacts on marine ecosystems. *Ann. Rev. Mar. Sci.* **4**, 11–37 (2012), 10.1146/annurev-marine-041911-111611.
2. A. Borja, Grand challenges in marine ecosystems ecology. *Front. Mar. Sci.* **1**, 1 (2014), 10.3389/fmars.2014.00001.
3. G. B. Bonan, S. C. Doney, Climate, ecosystems, and planetary futures: The challenge to predict life in Earth system models. *Science* **359**, eaam8328 (2018), 10.1126/science.aam8328.
4. H. M. Benway *et al.*, Ocean time series observations of changing marine ecosystems: An era of integration, synthesis, and societal applications. *Front. Mar. Sci.* **6**, 393 (2019), 10.3389/fmars.2019.00393.
5. K. L. Smith Jr., *et al.*, Navigating the uncertain future of global oceanic time series. *Eos* **96** (2015), 10.1029/2015EO038095.
6. R. Danovaro *et al.*, Ecological variables for developing a global deep-ocean monitoring and conservation strategy. *Nat. Ecol. Evol.* **4**, 181–192 (2020), 10.1038/s41559-019-1091-z.
7. F. P. Chavez *et al.*, Climate variability and change: Response of a coastal ocean ecosystem. *Oceanography* **30**, 128–145 (2017), 10.5670/oceanog.2017.429.
8. B. H. Robison, K. R. Reisenbichler, R. E. Sherlock, The coevolution of midwater research and ROV technology at MBARI. *Oceanography* **30**, 26–37 (2017), 10.5670/oceanog.2017.421.
9. K. L. Smith Jr., *et al.*, Evolution of monitoring an abyssal time-series station in the northeast pacific over 28 years. *Oceanography* **30**, 72–81 (2017), 10.5670/oceanog.2017.425.
10. J. C. Field, R. C. Francis, Considering ecosystem-based fisheries management in the California Current. *Mar. Policy* **30**, 552–569 (2006), 10.1016/j.marpol.2005.07.004.

11. D. M. Checkley, J. A. Barth, Patterns and processes in the California Current system. *Prog. Oceanogr.* **83**, 49–64 (2009), 10.1016/j.pocean.2009.07.028.
12. R. W. El-Sabaawi, M. Trudel, D. L. Mackas, J. F. Dower, A. Mazumder, Interannual variability in bottom-up processes in the upstream range of the California Current system: An isotopic approach. *Prog. Oceanogr.* **106**, 16–27 (2012), 10.1016/j.pocean.2012.06.004.
13. F. Chenillat, P. Rivière, X. Capet, P. J. S. Franks, B. Blanke, California coastal upwelling onset variability: Cross-shore and bottom-up propagation in the planktonic ecosystem. *PLoS One* **8**, e62281 (2013), 10.1371/journal.pone.0062281.
14. M. Messié, F. P. Chavez, Seasonal regulation of primary production in eastern boundary upwelling systems. *Prog. Oceanogr.* **134**, 1–18 (2015), 10.1016/j.pocean.2014.10.011.
15. M. Messié, D. A. Sancho-Gallegos, J. Fiechter, J. A. Santora, F. P. Chavez, Satellite-based Lagrangian model reveals how upwelling and oceanic circulation shape krill hotspots in the California Current ecosystem. *Front. Mar. Sci.* **9**, 835813 (2022), 10.3389/fmars.2022.835813.
16. B. A. Black *et al.*, Winter and summer upwelling modes and their biological importance in the California Current Ecosystem. *Global Change Biol.* **17**, 2536–2545 (2011), 10.1111/j.1365-2486.2011.02422.x.
17. M. García-Reyes *et al.*, Integrated assessment of wind effects on central California's pelagic ecosystem. *Ecosystems* **16**, 722–735 (2013), 10.1007/s10021-013-9643-6.
18. R. R. Rykaczewski, D. M. Checkley, Influence of ocean winds on the pelagic ecosystem in upwelling regions. *Proc. Natl. Acad. Sci. U.S.A.* **105**, 1965–1970 (2008), 10.1073/pnas.0711777105.
19. W. J. Sydeman *et al.*, Climate change and wind intensification in coastal upwelling ecosystems. *Science* **345**, 77–80 (2014), 10.1126/science.1251635.
20. R. R. Rykaczewski *et al.*, Poleward displacement of coastal upwelling-favorable winds in the ocean's eastern boundary currents through the 21st century. *Geophys. Res. Lett.* **42**, 6424–6431 (2015), 10.1002/2015gl064694.
21. Y. Pan *et al.*, Research progress in artificial upwelling and its potential environmental effects. *Sci. China Earth Sci.* **59**, 236–248 (2016), 10.1007/s11430-015-5195-2.
22. E. Di Lorenzo, M. D. Ohman, A double-integration hypothesis to explain ocean ecosystem response to climate forcing. *Proc. Natl. Acad. Sci. U.S.A.* **110**, 2496–2499 (2013), 10.1073/pnas.1218022110.
23. A. Barton, F. G. Taboada, A. Atkinson, C. Widdicombe, C. Stock, Integration of temporal environmental variation by the marine plankton community. *Mar. Ecol. Prog. Ser.* **647**, 1–16 (2020), 10.3354/meps13432.
24. P. van der Sleen *et al.*, Interannual temperature variability is a principal driver of low-frequency fluctuations in marine fish populations. *Commun. Biol.* **5** (2022), 10.1038/s42003-021-02960-y.
25. A. Hastings, C. L. Hom, S. Ellner, P. Turchin, H. C. J. Godfray, Chaos in ecology: Is mother nature a strange attractor? *Annu. Rev. Ecol. Evol. Syst.* **24**, 1–33 (1993), 10.1146/annurev.es.24.110193.000245.
26. H. Hoving, B. Robison, The pace of life in deep-dwelling squids. *Deep Sea Res. Part I* **126**, 40–49 (2017), 10.1016/j.dsr.2017.05.005.
27. S. Ralston, J. C. Field, K. M. Sakuma, Long-term variation in a central California pelagic forage assemblage. *J. Mar. Syst.* **146**, 26–37 (2015), 10.1016/j.jmarsys.2014.06.013.
28. H. A. Ruhl, K. L. Smith, Shifts in deep-sea community structure linked to climate and food supply. *Science* **305**, 513–515 (2004), 10.1126/science.1099759.
29. L. A. Kuhnz, H. A. Ruhl, C. L. Huffard, K. L. Smith, Benthic megafauna assemblage change over three decades in the abyss: Variations from species to functional groups. *Deep Sea Res. Part II* **173**, 104761 (2020), 10.1016/j.dsr2.2020.104761.
30. K. L. Smith Jr., *et al.*, Large salp bloom export from the upper ocean and benthic community response in the abyssal northeast Pacific: Day to week resolution. *Limnol. Oceanogr.* **59**, 745–757 (2014), 10.4319/lo.2014.59.3.0745.
31. C. L. Huffard, L. A. Kuhnz, L. Lemon, A. D. Sherman, K. L. Smith, Demographic indicators of change in a deposit-feeding abyssal holothurian community (station M, 4000m). *Deep Sea Res. Part I* **109**, 27–39 (2016), 10.1016/j.dsr.2016.01.002.
32. R. Baldwin, R. Glatts, K. Smith, Particulate matter fluxes into the benthic boundary layer at a long time-series station in the abyssal NE Pacific. *Deep Sea Res. Part II* **45**, 643–665 (1998), 10.1016/s0967-0645(97)00097-0.
33. K. L. Smith Jr., H. A. Ruhl, C. L. Huffard, M. Messié, M. Kahru, Episodic organic carbon fluxes from surface ocean to abyssal depths during long-term monitoring in NE Pacific. *Proc. Natl. Acad. Sci. U.S.A.* **115**, 12235–12240 (2018), 10.1073/pnas.1814559115.
34. C. A. Choy, S. H. D. Haddock, B. H. Robison, Deep pelagic food web structure as revealed by in situ feeding observations. *Proc. Royal Soc. B.* **284**, 20172116 (2017), 10.1098/rspb.2017.2116.
35. E. Di Lorenzo *et al.*, North Pacific Gyre Oscillation links ocean climate and ecosystem change. *Geophys. Res. Lett.* **35**, L08607 (2008), 10.1029/2007GL032838.
36. N. J. Mantua, S. R. Hare, Y. Zhang, J. M. Wallace, R. C. Francis, A Pacific interdecadal climate oscillation with impacts on salmon production. *Bull. Amer. Meteor. Soc.* **78**, 1069–1079 (1997), 10.1175/1520-0477(1997)078<1069:APICOW>2.0.CO;2.
37. F. Chenillat, P. Rivière, X. Capet, E. Di Lorenzo, B. Blanke, North Pacific Gyre Oscillation modulates seasonal timing and ecosystem functioning in the California Current upwelling system. *Geophys. Res. Lett.* **39**, L01606 (2012), 10.1029/2011GL049966.
38. K. L. Smith Jr., *et al.*, Climate, carbon cycling, and deep-ocean ecosystems. *Proc. Natl. Acad. Sci. U.S.A.* **106**, 19211–19218 (2009), 10.1073/pnas.0908322106.
39. F. P. Wilkerson, A. M. Lassiter, R. C. Dugdale, A. Marchi, V. E. Hogue, The phytoplankton bloom response to wind events and upwelled nutrients during the CoOP WEST study. *Deep Sea Res. Part II* **53**, 3023–3048 (2006), 10.1016/j.dsr2.2006.07.007.
40. M. García-Reyes, J. L. Largier, W. J. Sydeman, Synoptic-scale upwelling indices and predictions of phyto- and zooplankton populations. *Prog. Oceanogr.* **120**, 177–188 (2014), 10.1016/j.pocean.2013.08.004.
41. R. C. Zimmerman, J. N. Kremer, R. C. Dugdale, Acceleration of nutrient uptake by phytoplankton in a coastal upwelling ecosystem: A modeling analysis. *Limnol. Oceanogr.* **32**, 359–367 (1987), 10.4319/lo.1987.32.2.0359.
42. M. Messié, F. P. Chavez, Nutrient supply, surface currents, and plankton dynamics predict zooplankton hotspots in coastal upwelling systems. *Geophys. Res. Lett.* **44**, 8979–8986 (2017), 10.1002/2017GL074322.
43. O. N. Bjørnstad, R. M. Nisbet, J.-M. Fromentin, Trends and cohort resonant effects in age-structured populations. *J. Anim. Ecol.* **73**, 1157–1167 (2004), 10.1111/j.0021-8790.2004.00888.x.
44. L. W. Botsford, M. D. Holland, J. C. Field, A. Hastings, Cohort resonance: A significant component of fluctuations in recruitment, egg production, and catch of fished populations. *ICES J. Mar. Sci.* **71**, 2158–2170 (2014), 10.1093/icesjms/fsu063.
45. K. MacKenzie, D. Robertson, J. Adams, A. Altieri, B. Turner, Structure and nutrient transfer in a tropical pelagic upwelling food web: From isoscapes to the whole ecosystem. *Prog. Oceanogr.* **178**, 102145 (2019), 10.1016/j.pocean.2019.102145.
46. F. P. Chavez, M. Messié, A comparison of eastern boundary upwelling ecosystems. *Prog. Oceanogr.* **83**, 80–96 (2009), 10.1016/j.pocean.2009.07.032.
47. T. Miller, R. Brodeur, G. Rau, K. Omori, Prey dominance shapes trophic structure of the northern California Current pelagic food web: Evidence from stable isotopes and diet analysis. *Mar. Ecol. Prog. Ser.* **420**, 15–26 (2010), 10.3354/meps08876.
48. P. E. Caiger, L. S. Lefebve, J. K. Llopiz, Growth and reproduction in mesopelagic fishes: A literature synthesis. *ICES J. Mar. Sci.* **78**, 765–781 (2021), 10.1093/icesjms/fsaa247.
49. G. Vogt, A compilation of longevity data in decapod crustaceans. *Nauplius* **27** (2019), 10.1590/2358-2936e2019011.
50. K. Hüssy *et al.*, Challenging ICES age estimation protocols: Lessons learned from the eastern Baltic cod stock. *ICES J. Mar. Sci.* **73**, 2138–2149 (2016), 10.1093/icesjms/fsw107.
51. G. Cailliet *et al.*, Age determination and validation studies of marine fishes: Do deep-dwellers live longer? *Exp. Gerontol.* **36**, 739–764 (2001), 10.1016/s0531-5565(00)00239-4.
52. A. Z. Worden, J. K. Nolan, B. Palenik, Assessing the dynamics and ecology of marine picophytoplankton: The importance of the eukaryotic component. *Limnol. Oceanogr.* **49**, 168–179 (2004), 10.4319/lo.2004.49.1.0168.
53. R. W. Eppley, F. H. Reid, J. R. Strickland, "Estimates of phytoplankton crop size, growth rate, primary production" in *The ecology of the plankton off La Jolla, California in the period April through September, 1967*, J. D. H. Strickland, Ed. (University of California Press, 1970), pp. 33–42, https://escholarship.org/uc/item/4q01m9gk.
54. J. R. Beers, G. L. Stewart, "Numerical abundance and estimated biomass of microzooplankton" in *The ecology of the plankton off La Jolla, California, in the period April through September, 1967*, (University of California Press, 1970), pp. 67–87, https://escholarship.org/uc/item/4q01m9gk.
55. B. Schlining, N. Stout, MBARI's video annotation and reference system. *OCEANS 2006* (2006), 10.1109/oceans.2006.306879.
56. B. H. Robison, K. R. Reisenbichler, R. E. Sherlock, Giant larvacean houses: Rapid carbon transport to the deep sea floor. *Science* **308**, 1609–1611 (2005), 10.1126/science.1109104.
57. K. Katija, R. E. Sherlock, A. D. Sherman, B. H. Robison, New technology REVEALS the role of giant larvaceans in oceanic carbon cycling. *Sci. Adv.* **3**, e1602374 (2017), 10.1126/sciadv.1602374.
58. L. Lauerman, R. Kaufmann, K. Smith, Distribution and abundance of epibenthic megafauna at a long time-series station in the abyssal northeast Pacific. *Deep Sea Res. Part I* **43**, 1075–1103 (1996), 10.1016/0967-0637(96)00045-3.
59. W. W. Wakefield, W. Smithey, *Two Camera Sleds for Quantitative Study of Deep-Sea Megafauna* (Scripps Institution of Oceanography, La Jolla, California, USA, Reference Series No. 89–14, 1989).
60. L. A. Kuhnz, H. A. Ruhl, C. L. Huffard, K. L. Smith Jr., Rapid changes and long-term cycles in the benthic megafaunal community observed over 24 years in the abyssal northeast Pacific. *Prog. Oceanogr.* **124**, 1–11 (2014), 10.1016/j.pocean.2014.04.007.
61. G. R. North, T. L. Bell, R. F. Cahalan, F. J. Moeng, Sampling errors in the estimation of empirical orthogonal functions. *Mon. Weather Rev.* **110**, 699–706 (1982), 10.1175/1520-0493(1982)110<0699:SEITEO>2.0.CO;2.
62. W. G. Large, S. Pond, Open ocean momentum flux measurements in moderate to strong winds. *J. Phys. Oceanogr.* **11**, 324–336 (1981), 10.1175/1520-0485(1981)011%3C0324:OOMFMI%3E2.0.CO;2.
63. B. J. Pyper, R. M. Peterman, Comparison of methods to account for autocorrelation in correlation analyses of fish data. *Can. J. Fish. Aquat. Sci.* **55**, 2127–2140 (1998), 10.1139/f98-104.
64. J. W. White *et al.*, Transient responses of fished populations to marine reserve establishment. *Conserv. Lett.* **6**, 180–191 (2013), 10.1111/j.1755-263x.2012.00295.x.
65. M. Messié *et al.*, Data from: Coastal upwelling drives ecosystem temporal variability from the surface to the abyssal seafloor. Zenodo. https://doi.org/10.5281/zenodo.7651067. Deposited 7 March 2023.
66. M. Messié, Code for: Coastal upwelling drives ecosystem temporal variability from the surface to the abyssal seafloor. Zenodo. https://doi.org/10.5281/zenodo.7651348. Deposited 17 February 2023.